J Electr Eng Technol Vol. 9 No. 1: 259-267, 2014
http://dx.doi.org/10.5370/JEET.2014.9.1.259

ISSN(Print) 1975-0102
ISSN(Online) 2093-7423

A New Reliable Algorithm for Identifying Types of Partial Discharge Detected through Ultrasonic Emission

Mohammad Shukri Hapeez†, Ngah Ramzi Hamzah *, Habibah Hashim * and Ahmad Farid Abidin*

Abstract – This paper presents a simple, consistent and reliable technique to identify detected partial discharges (PD) using an acoustic ultrasonic method. A new reliable algorithm named 'Simple Partial Discharge Identifier' (SPDI) is proposed to perform identification process of the detected ultrasonic signals of PD. Experimental works based on recommended practices were setup and the ultrasonic signals of the PD were recorded. The PD data is then employed as the reference data. The SPDI developed has been tested against commonly used models in Neural Network (NN). Results from the SPDI algorithm shows more reliable results compared to NN models results. Comparison made on the mean square error (MSE) results shows SPDI produces the desired outcome with lower MSE in 97.17% of trials. Low error of SPDI indicates a high reliability to be applied in the identification of PD.

Keywords: Partial Discharge, SPDI, Identification, Acoustic Emission

1. Introduction

The insulation material of electrical power equipment will gradually deteriorate after a long period of time, causing partial discharge (PD) phenomena to occur which will eventually lead to complete insulation breakdown [1-2]. For this reason, detecting partial discharge is useful for the insulation assessment and to predict the life of the insulation [1-2, 3-16].

In general, there are two methods in detecting PD which are non-electrical (non-contact) method or electrical method [1-4, 8]. The electrical method usually uses impedance to measure the voltage impulse, and coupling capacitor to measure the current impulse and apparent charge. The non-contact method usually uses chemical transformation, gas pressure, heat, light and acoustic emission. However, only the last two are considered as practically important [15]. In order to provide the accurate solution, it is vital to identify the PD type first. By identifying and determining the PD characteristic, further analysis can be performed and solutions can be proposed. Various methods have been proposed for the identification of PD types. However, if the PD is not visible to the human vision, recognition of the PD type will be difficult to perform. It would be of much easier to make identification if the signal can be made to be visible to the eyes.

There are many tools or methods commonly used to identify PD types such as Neural Network (NN), Machine Learning (ML) and Support Vector Machine (SVM) [4, 6-7 and 9-11]. Even though the most preferred tools are NN, there are issues that diminish the advantages of NN. NN can be considered as a black-box model and the users practically do not know the content of the black-box [5].

The black-box behaviour of NN and the reliability problem of learning interference are the common difficulties in using NN [4, 6-7 and 9-11]. An overview of NN disadvantages will be described in details, later in the methodology section. The SPDI algorithm was developed in response to the pre-determined inadequacies of NN in producing highly reliable results with respect to the identification of PDs. The advantages of the SPDI algorithm are its reliability and its ability to deliver accurate results despite being a non-complex, transparent algorithm which does not rely on commercial software tools or models. Also, it does not pose serious issues of consistencies found in other method. Experimental works have been conducted in accordance to existing standards [17-20] and the obtained data has been validated to ascertain reliability of the experimental work.

2. Experimental Works and Data Verification

In the experimental work, a device called acoustic ultrasonic detector is used to record and store the acoustic PD signals. The ultrasonic detector has the frequency range from 20 kHz to 100 kHz and the central frequency of 40 kHz is applied in this work, similar to that used by others [1-2, 6-8]. The diagram of the non-contact method applied in this work is shown in Fig. 1(a). The setup of the experimental work for capturing PD ultrasonic signals is

† Corresponding Author: Faculty of Electrical Engineering, University Teknologi MARA, Malaysia, Malaysia. (shukri@ieee.org)
* Faculty of Electrical Engineering, University Teknologi MARA, Malaysia, Malaysia. ({ngahramzi, ibah350, ahmad924}@salam.uitm.edu.my)
Received: August 30, 2012; Accepted: August 2, 2013

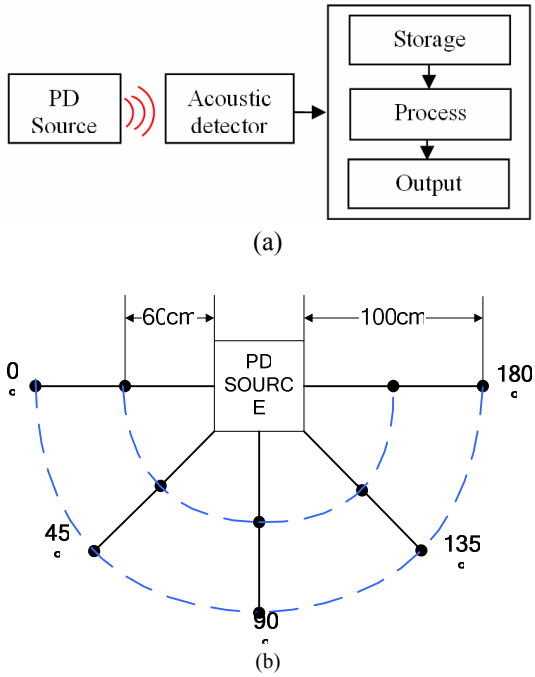

Fig. 1. (a) Overview of the non-contact method applied in this study;. (b) The location arrangement of the ultrasonic acoustic device.

shown in Fig. 1(b). The ultrasonic probe is placed 60cm to 100cm in front of the test object in order to obtain clear response of acoustic signal. The PD source is generated by various electrodes arrangement that will be the described in section 2.1. A test circuit consisting of transformer is connected to the PD source via coaxial cable.

From the observation, the maximum distance that the acoustic signals can be clearly measured is at 60cm. The corresponding angle measurement are located at 0°, 45°, 90°, 135° and 180°. However, the angle position does not have any significant effect on the acoustic signal. Also, it has been verified that the cable does not produce significant noise to the recorded ultrasonic signal. The following procedures of the experimental works are mostly referred to standards [17-20] and publication [1-2, 6-8, 15-16].

Step 1: The acoustic signal of the PD source is measured using the ultrasonic device placed 60cm from the PD source. The measured data will be converted into signal waveform.

Step 2: By using wavelet de-noising method, noise occurrence on the signal is eliminated from the PD signal waveform.

Step 3: The converted PD waveform graph is plotted with the power source waveform. The phase location of the acoustic PD signals will be aligned with those of the power source waveform.

Step 4: From the plotted waveform, the discharge angles are determined. Then, the types of the discharge are classified.

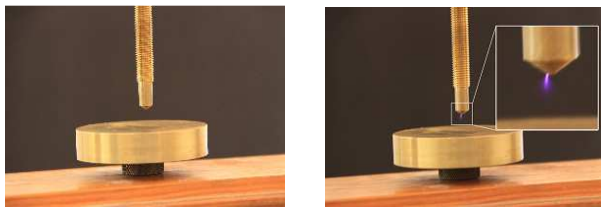

(a) (b)

Fig. 2. (a) The apparatus setup for the corona discharge. (b) The occurrence of the corona discharge.

2.1 Operation setup and process

The setups of apparatus for producing different types of PD are shown in Fig.2 through Fig. 4. The apparatus is supplied via a transformer and cable. On the occurrence of the PD the acoustic detector detect the sound produced by the PD and store it into a sound format file. The sound file format then is converted into waveform using MATLAB software.

2.1.1 Corona Discharge

The corona discharge was produced by using a brass needle and brass plate as shown in Fig. 2 (a). The high voltage brass needle points towards a grounded brass plate. The gap was tested at 3mm, then at 4.5mm, 6mm, 7.5mm 9mm and 10mm. The applied voltages were varied from 3kV to 11.5kV at increments of 0.5kV. Voltages of more than 11.5kV will cause arc bridging across top and bottom electrodes, leading to complete breakdown. As the gap increases, the voltage injected needed to be increased. This is because the larger air gap increases the insulation between the electrodes, hence a higher voltage is required to ionize the air and transfer its charges to the other electrode.

The corona discharges occur at the gap of 7.5mm and voltages in the region of 9.5kV to 11.5kV. The corona discharges as can be seen in Fig 2 (b).

2.1.2 Void Discharge

For internal discharges, electrodes of the same size as shown in Fig. 3 (a) are used. Perspex with air void created during moulding was used in the experiment to produce internal discharges. The perspex size is customized to be slightly larger than the electrodes. The dimension of the perspex is shown in Fig. 3 (a) with air void of size approximately 1 to 2 mm.

An air-tight vessel that is able to withstand high voltage was used as shown in Fig 3 (a). The vessel is set at a pressure of -0.8bar. Partial discharges occur as shown in Fig. 3(b) when the voltage is in the range of 12.5kV to 13kV. At this point, the discharges occurring could be purely internal or coupled with surface discharge. It has been reported that an air tight condition is necessary in

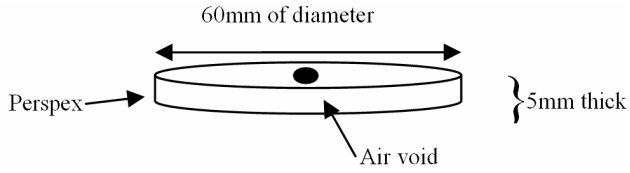

(a)

(b)

Fig. 3. (a) The dimension and type of the specimen used including the air void. (b) The apparatus setup for the internal discharge. (b) The occurrence of the internal discharge.

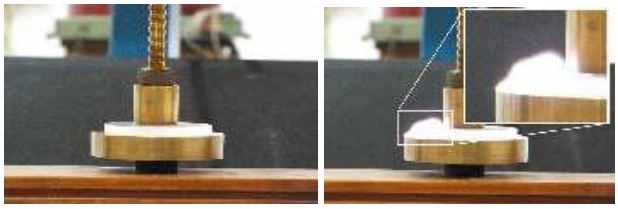

(a) (b)

Fig. 4. (a) The apparatus setup for the surface discharges. (b) The occurrence of surface discharge.

order to prevent occurrence of surface discharge [9]. An experiment has been conducted to test if the air-tight condition i.e. not at room pressure, can affect the breakdown voltage.

As mentioned earlier, results reported in well cited publications will be used as references in the validation process of the determination of the type of discharges that occur. Complete breakdown will follow if the voltage injected higher than 13kV.

2.1.3 Surface Discharge

For surface discharges, the top electrode is relatively smaller than the bottom electrode. Perspex is used as the insulation material and is placed in between the two brass electrode as shown in Fig. 4(a). The top electrode is injected with high voltage and the bottom electrode is connected to ground.

The perspex is placed on top of the bottom electrode and the top electrode will be firmly placed on top of the perspex. The aim is to force the discharge to be arcing on the surface of the perspex. Voltage is applied to the top electrode; starting at 1kV with 1kV increment. Between 9kV to 10kV, the ultrasonic sound of the surface discharge can be detected. The surface discharge is shown in Fig. 4 (b). Complete breakdown will occur when the voltage is over 10kV.

2.2 Data validation and verification

In order to validate the obtained acoustic PD data, comparison with standards and other existing techniques as published in [1, 2, 6-8 and 17-20] has been conducted. Using the power source signal as the reference, the acoustic PD data generated from the corona discharge experiment is displayed in a phase-resolved plot. Fig. 5(a) shows the plot of the generated acoustic data from the experiment and Fig. 5(b) shows the standard plot of the phase-resolved corona discharge [1, 2, 6-8 and 17-20].

Comparing the two plots, it can be seen that the signals concentrate at 270°. Fig. 5(b) also shows that there are discharges at 90°. This only occurs when the discharge phenomenon is very intense. In this work, the discharge is at typical conditions; hence the discharge signal is not visible at 90°. As a result, the plots shown in Fig. 5(a) can be verified as a valid corona discharge signal, under typical condition. The phase-resolved plots of the obtained surface discharge signals are shown in Fig. 6. Fig 6(a) shows the signals obtained experimentally and Fig. 6(b) shows the signals mentioned in reviews [1, 2, 6, 8 and 17-20]. It can be seen that for both plots, the signals concentrate at 90° and at 270°. Thus it can be verified that the signals shown in Fig. 6(a) as valid surface discharge signal.

The phase-resolved plots of the obtained internal discharge signals are shown in Fig. 7(a) and the phase-resolved of the surface discharge signal based on [1, 2, 6, 8 and 17-20] is shown in Fig. 7(b). The internal discharge

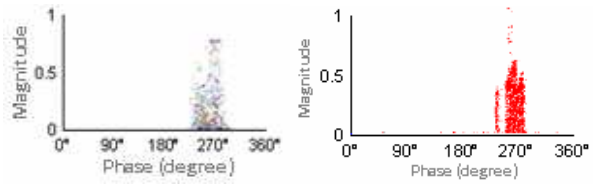

(a) (b)

Fig. 5. The comparison of the phase-resolved partial discharge of the corona discharges obtained from the experimental work (a) against reference (b).

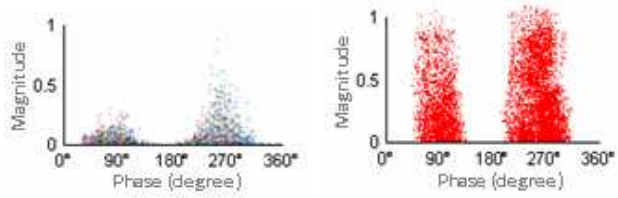

(a) (b)

Fig. 6. The comparison of the phase-resolved partial discharge of the surface discharges obtained from the experimental work (a) against reference (b).

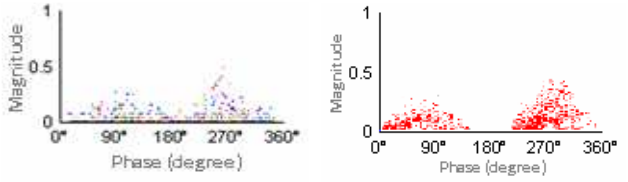

(a) (b)

Fig. 7. The comparison of the phase-resolved partial discharge of the internal discharges obtained from the experimental work (a) against reference (b).

signals concentrate at 270° and slightly appear at 90°.

It may appear that the phase-resolved plot of the internal discharges (Fig. 7) is similar to that of surface discharges. However, a closer examination reveals that the internal discharges plot has a slightly lower magnitude. Also the scatter of the internal discharges plot extends to wider angles range.

3. Methodology for Comparison

MATLAB software is used for processing the data and for the development of the NN models. In order to prove the reliability problem associated with the NN models, the SPDI was developed to improve the reliability problems of the NN models. Its effectiveness is investigated by comparing its results against the results of NN models. For NN, five models were used; the NN pattern recognition (NNPR), the Multi-Layer Perceptron NN (MLPNN), Radial Basis Function NN (RBFNN), Bayesian RBFNN (BRBFNN) and Probabilistic NN (PNN). Parameters for all models have been configured to suit the experiment in order to obtain the optimised results out of NN. The reference sets are used as the training set to train the NN. The Mean Square Error (MSE) of all NNPR, MLPNN, RBFNN, BRBFNN and PNN will be obtained and will be used to compare against the MSE obtained from SPDI algorithm. The data used are randomly exchanged against other sets in order to analyse the consistency of the results produced by SPDI and NN models. The response from the NN models on the input is taken to calculate the MSE against the reference signals. Based on these responses from the NN models, the identified input can be recognized. For each iteration performed, the NN models produce different responses to the reference signals. The consistency of the response is imperative in determining the results produced.

The verified data from the experimental work is used in this comparison work. Two data sets will be selected to be used as references and the signal to be identified. The selected set is used as the references and the acoustic PD data input on all SPDI, NNPR, MLPNN, RBFNN, BRBFNN and PNN techniques as shown in Fig. 8.

In order to recognise the difference between the

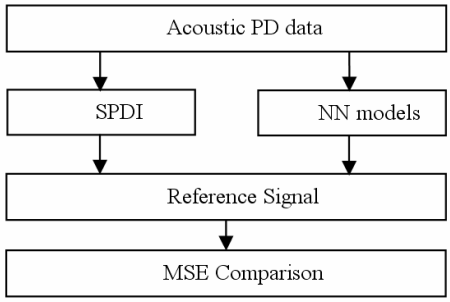

Fig. 8. A flowchart showing the methodology to compare the performance of the algorithms of SPDI

references signals against the identified signals, MSE will be employed. MSE defines the minimum error state of each model. Lower MSE values indicate that the identified results of the identification process are more accurate. The identification reliability can be evaluated to determine the trustworthiness of the employed methods or algorithms.

3.1 Overview of NN

NN has been used in many fields and can be considered as the preferred tool. Proponents of the NN are unlikely to mention the handicaps of the NN models that render the NN as disadvantageous. NN can be considered as a black-box model of which users practically have no knowledge of the content of the black-box [5]. The black-box yields uncertain behaviour in terms of reliability and consistency of learning interference and this renders its incompetence for use [4-6]. Various methods proposed by researchers tend to use NN models and improvise the current models to more advanced models and produce better outcome. With this trend, only the developers fully comprehend their inner working but not to others made reference to the publications. The training outcome can be non-deterministic and depend crucially on the choice of initializing parameters. NN can be contemplated as not suitable for problem understanding. Other mathematical methods or some nonlinear derivatives can be used as a solver because users can see the content of the process. In NN environment, users have limitation in setting up the NN and in determining the neurons and the hidden layers of the network, but still unable to determine what happen in the black box of NN. NN use the neuron to learn and the learning process makes the neural network intelligent enough to understand data patterns to make decision. NN training process is by repeatedly presenting data to the NN model. The NN will then adjust its parameters slightly to represent the new data better. When a new set of data in one region of the input is repeatedly presented, the NN can forget the learned mapping in other regions of the input. This situation is referred to as interference problem. The forgetting behaviour can be useful if the function modelled is changing over time, because the new data will eventually erase the effects of

the obsolete input.

3.2 Comparison procedure

The workflow of the whole procedure where the SPDI algorithm and NN models are used as comparison within the process is shown as a flowchart in Fig. 9. The steps involved in the flowchart are described in the following:

i) Define the reference – after the experimental work has been completed, PD source signals are recorded and stored in MATLAB.

ii) De-noise (Wavelet) – the acoustic PD data is de-noised by using wavelet based de-noising method. The selection of mother wavelet has been tested earlier in order to select which type is better and to ensure no PD signals are left out. Discrete Wavelet Transform (DWT) shows good results have been selected to be used with 'db3' for the ideal performance in suppressing the PD noise. The signal will be decomposed; the filtering process applied and the signal reconstructed to minimize the loss of the original signal. And by determining the exact thresholding parameter to the noisy signals it is expected to provide better de-noising effect to the noisy PD signals.

iii) SPDI algorithm – the acoustic PD data is processed with the SPDI algorithm.

iv) NN models – for comparison purpose, similar acoustic PD data used by the SPDI will also be used by the NN models. The parameters for the NNPR, MLPNN, RBFNN, BRBFNN and PNN have been configured for optimum performance in producing the best results. The number of neurons and the hidden layer are set at an optimal number.

v) MSE Comparison – after the acoustic PD data has been processed by both techniques, the MSE results from both techniques will be produced. The MSE can be described by the equation in (1).

$$\overline{X} = \frac{1}{n}\sum_{i=1}^{n}(xi) \tag{1}$$

vi) Analysis results from both methods – after obtaining the MSE values for both techniques, the comparison will be made. The lowest MSE values from either of both techniques can be used to identify the type of PD by making comparison to the defined reference. The lowest MSE from the defined reference set indicates that the input signal have low residual and high signal pattern similarity for that reference, hence can be used to identify the PD type.

3.3 Working principle of SPDI algorithms

It is not an easy task to identify and characterize from the recurring pattern of the obtained acoustic signals, and

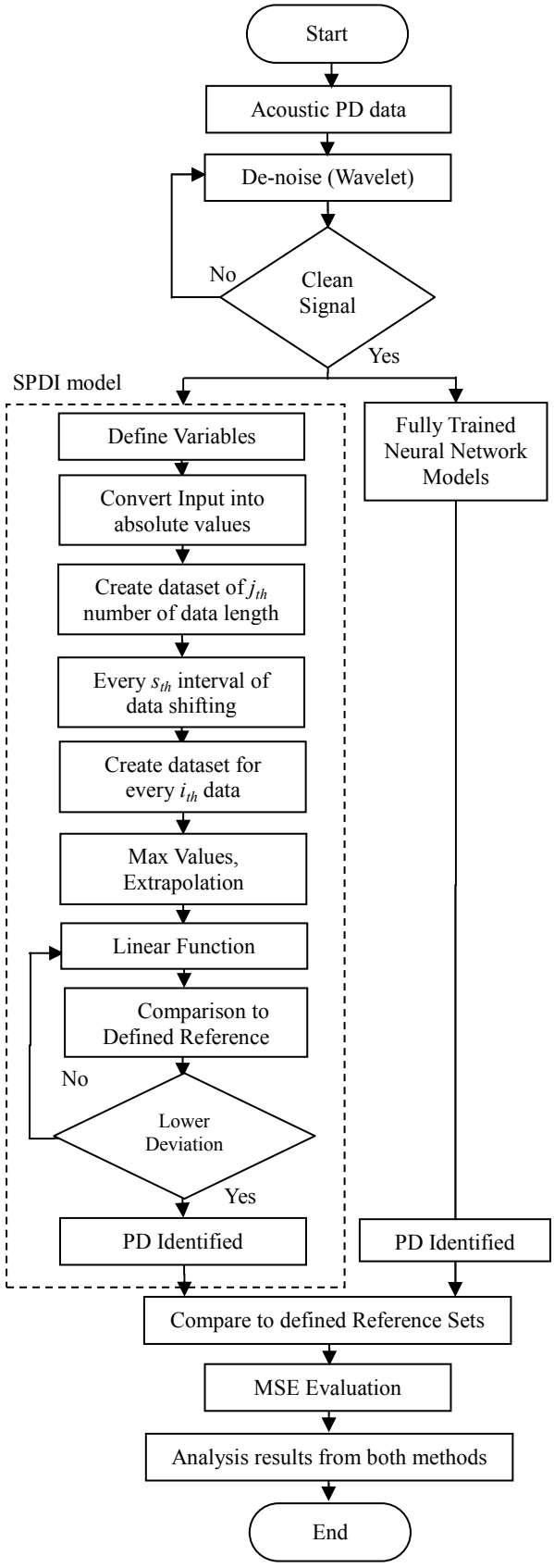

Fig. 9. The flowchart of the whole working process. The dotted box area is the new proposed SPDI algorithm

SPDI was constructed specifically for this purpose. Theoretically, SPDI is an algorithm constructed using mathematical models, with an emphasis given to simple and transparent structure compared to NN.

The diagram of the flowchart for the SPDI algorithm operation is depicted in Fig. 8. The following is the SPDI algorithm description:

Step 1: Define variables – the values for the following variables will be defined in order to use it for the parameter of the algorithm.

i = Number of data
j = Number of datasets
s = Interval length shifting

Step 2: Convert acoustic PD data input into absolute values – the input values is converted into absolute values (positive values) before it is used in the identification process. The purpose is that only positive values that will be used in SPDI algorithm, hence, the negative values can be used to fill the positive data in order to pack the input signals on the positive side to ease the curving fitting process on the next step.

Step 3: Create j number of dataset of length i – from the input data, create a dataset that contain i number of data in that one particular set of data. The i is the variable for number of data which has been defined in Step 1.

Step 4: Define the s_{th} data shifting – after one set of data created, another set will be created with the same number of length of data set as previous set. The selection of the dataset starts after shifting to the defined s in Step 1. The second dataset contain data starting from s_{th} position in the input, with j_{th} number of length.

Step 5: Create set of j_{th} dataset – the set of data comprises the number of dataset exist in the input. Step 3 and Step 4 will be repeated until the last data in the input is taken into account.

Step 6: Max Values, Extrapolation – each data set will go through max values process and each of the data set and the reference set will go through the extrapolation process. The Max values is process is when a single dataset will be evaluated for its maximum value from the 0 coordinates of Y axis. The maximum values accumulated will then be extrapolated. The extrapolation can be described as shown in (2). Every dataset and references set will be extrapolate.

$$y(x_n) = y_{k-1} + \frac{x_n - x_{k-1}}{x_k - x_{k-1}}(y_k + y_{k-1}) \quad (2)$$

Step 7: Linear Function – after Step 6 completed, the dataset will be fitted to a curve. The curve fitting method will be used in this process. The linear curve fitting is based on the equation depicted in (3). In order to adjust the curve created to get much lower MSE, the signal value for extrapolation function and linear function can be regulate as desired. In this work, a fixed value has been used in order to minimize the potential error and to stabilize each successive error generated.

$$f(x) = a_n x_n + a_{n-1} x_{n-1} + \cdots + a_1 x_1 + c \quad (3)$$

Step 8: PD Identification – After Step 7 is completed, the PD type can be identified from the defined dataset that have the lowest MSE values.

4. Results

The SPDI technique was developed in providing most reliable and consistent results in identifying types of PD signals.

The comparison of the results using SPDI, NNPR, MLPNN, RBFNN, BRBFNN and PNN are presented in Fig. 10 through 12. The plotted graphs represent the 40 successive experiments conducted on all PD types. SPDI shows almost consistent MSE. The MSE of SPDI can be seen as a straight line because the deviations for all experiments are low.

Fig. 10 shows the plotted graph of the MSE results obtained from SPDI and the NN models for corona discharges.

The SPDI algorithm shows reliable results as the MSE on all 40 consecutive experiments show almost similar error. For NNPR and MLPNN techniques, the MSE result of both shows an inconsistency compared to SPDI. The NNPR pattern of learning shows an understanding of the pattern learned and came close to the SPDI on a few occasion, at the 4th, 8th, 27th and 40th experiment but produce high MSE between the 9th and 26th experiments. The MLPNN shows high MSE initially, but perform better

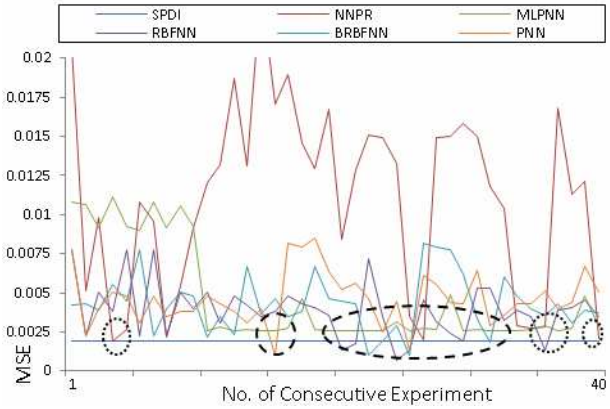

Fig. 10. The plotted results of 40 consecutive experiments of the SPDI, NNPR and MLP to identify corona discharge signal. The dotted circles show the points where MSE of NN models are better than SPDI.

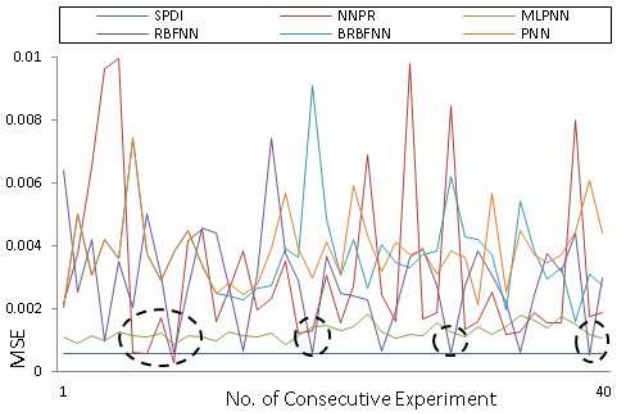

Fig. 11. The plotted results of 40 consecutive experiments of the SPDI, NNPR and MLPNN to identify surface discharge signal. The dotted circle shows the MSE of NN models better than SPDI.

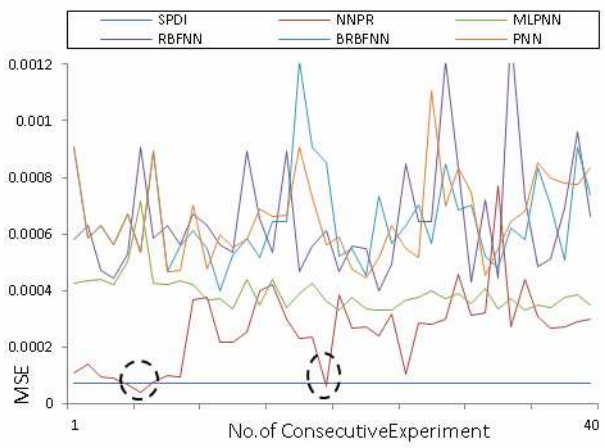

Fig. 12. The plotted results of 40 consecutive experiments of the SPDI, NN and MLP to identify internal discharge signal. The dotted circles show the points where MSE of NN models are better than SPDI.

from 10th experiment onward, the MSE is lower and close to SPDI but still SPDI produces much lower MSE.

Capitalizing on the presented results of the plotted MSE, an outcome has been summarized and tabulated in Table 1. From Table 1, it can be further derived that the SPDI was able to provide lowest MSE in 86.7% in the experiments conducted on all PD types. The NNPR model scored 3.3% of lowest MSE in the experiment. MLPNN was unable to provide any lowest MSE while PNN contributes to only 0.8% of lowest MSE from the experiments conducted. RBFNN and BRBRNN were able to deliver lowest MSE in the experiment conducted by only 5.8% and 3.3%, respectively.

Overall, the amount of run-time process of the SPDI algorithm is very much less than that of NN models. The parameters and the process of the SPDI algorithm are transparent and can be amended, as it is not based on black-box model concept.

Table 1. Percentage of lowest MSE scored by the models in 40 experiments involving all PD types.

Models	PD Type			All PD Type
	Corona	Internal	Surface	
SPDI	75%	92.5%	92.5%	86.7%
NNPR	0%	7.5%	2.5%	3.3%
MLPNN	0%	0%	0%	0%
RBFNN	12.5%	0%	5%	5.8%
BRBFNN	10%	0%	0%	3.3%
PNN	2.5%	0%	0%	0.8%

5. Conclusion

This study proposes the SPDI method of identifying types of PD detected by acoustic emission. The validation of the acoustically generated PD data and the classification of the PD data into the various types using the proposed novel algorithm were presented. The classification of the measured PD data obtained using NN models and the SPDI algorithm were analyzed and a comparison of each models' reliability based on MSE were carried out. From the results obtained, conclusions were made over the advantages and disadvantages of SPDI and NN models with respect to their ability to deliver reliable results. The SPDI algorithm was able to produce more reliable, consistent and better results in 97.17% of experiments (from all PD types) with lower MSE against the NN models. From the presented work, it can be further concluded that a simpler method such as SPDI can be used to provide better results compared to other complex and rigorous methods.

Acknowledgements

Support from Universiti Teknologi MARA, Kementerian Pengajian Tinggi (KPT) Malaysia for Mybrain15 (myphd), ERGS Grant (600-RMI/ERGS 5/3 (20/2012)) and Mustafar Kamal Hamzah, are gratefully acknowledged and appreciated for the implementation of this project.

References

[1] Li-Jung Chen, Whei-Min Lin, Ta-Peng Tsao and Yu-Hsun Lin, "*Study of Partial Discharge Measurement in Power Equipment Using Acoustic Technique and Wavelet Transform*", IEEE Trans. Power Delivery, Vol. 22, No. 3, July 2007.

[2] Li-Jung Chen, Ta-Peng Tsao and Yu-Hsun Lin, "*New Diagnosis Approach to Epoxy Resin Transformer Partial Discharge Using Acoustic Technology*", IEEE Trans. Power Delivery, Vol. 20, No. 4, October 2005.

[3] IEEE Recommended Practice for the Detection of

Partial Discharge and the Measurement of Apparent Charge in Dry-type Transformers, IEEE Std., C56.124, 1992.

[4] IEEE Trial-Use Guide for the Detection of Acoustic Emissions from Partial Discharges in Oil-Immersed Power Transformer – Transformer Committee of the IEEE Power Engineering Society – Approved: 21 September 2000 – IEEE SA Standards Board.

[5] IEC 60270:2000 Standard, High Voltage Test Technique – Partial Discharge Measurement, 3rd edition, 2000.

[6] ASTM D3756-97 Standard Test Method for Evaluation to Resistance for Electrical Breakdown by Treeing in Solid Dielectric Materials Using Diverging Fields, 2010.

[7] Xin Liu, "*Partial Discharge Detection and Analysis in Low Pressure Environments*", Ph.D Thesis, The Ohio State University, USA, 2006.

[8] M. Conti, "*Development of Artificial Intelligence Systems for Electrical Insulation Defect Identification through Partial Discharge Measurement*", Ph.D Thesis, University of Bologna, Italy, 2003.

[9] M. Norgaard, O. Ravn, N. K. Poulsen, and L. K. Hansen, "*Neural networks for modeling and control of dynamic systems: A practitioner's handbook"*. London: Springer, 2000.

[10] W.R.Si, J.H.Li, D.J.Li, J.G.Yang and Y.M.Li, "*Investigation of a Comprehensive Identification Method Used in Acoustic Detection System for GIS*", IEEE Trans. Dielectrics and Electrical Insulation, Vol. 17, No. 3, June 2010.

[11] R.M. Sharkawy, T.K. Abdel-Galil, R.S. Mangoubi, M.M.Salama and R. Bartnikas, "*Particle Identification in Terms of Acoustic Partial Discharge Measurements in Transformer Oils*", IEEE Trans. Dielectrics and Electrical Insulation, Vol. 15, No. 6, December 2008.

[12] S.M. Markalous, S. Tenbohlen and K. Feser, "*Detection and Location of Partial Discharge in Power Transformers using Acoustic and Electromagnetic Signals*", IEEE Trans. Dielectrics and Electrical Insulation, Vol. 15, No. 6, December 2008.

[13] K.X. Lai, B.T. Phung and T.R. Blackburn, "*Application of Data Mining on Partial Discharge, Part I: Predictive Modelling Classification*", IEEE Trans. Dielectrics and Electrical Insulation, Vol. 17, No. 3, June 2010.

[14] V. M. Catterson, S. Bahadoorsingh, Susan Rudd, Stephen D.J. McArthur and Simon M. Rowland, "*Identifying Harmonic Attributes from Online Partial Discharge Data"*, IEEE Trans. Power Delivery, Vol. 26, No. 3, July 2011.

[15] T. Boczar, S. Borucki, A. Cichon and D. Zmarzly, "*Application Possibilities of Artificial Neural Networks for Recognizing Partial Discharges Measured by the Acoustic Emission Method*", IEEE Trans. Dielectrics and Electrical Insulation, Vol. 16, No. 1, February 2009.

[16] T. Pinpart and M.D. Judd, "*Differencing Between Partial Discharge Sources using Envelope Comparison of UHF Signals*", IET Science Measurement & Technology, Vol. 4, No. 5, 2010.

[17] X. Zhou, C. Zhou and I.J. Kemp, "*An Improved Methodology for Application of Wavelet Transform for Partial Discharge Measurement Denoising*", IEEE Trans. Dielectrics and Electrical Insulation, Vol. 12, No.3, June 2005.

[18] Z.S. Zhang and D.M. Xiao, "*Noise-based Wavelet Denoising Technique for Partial Discharge Measurement*", WSEAS Trans. Circuits and Systems, Issues 6, Vol. 7, June 2008.

[19] F.H. Kreuger, "*Partial Discharge Detection in High-Voltage Equipment*", Butterworth & Co. Publishers Ltd, 1989.

[20] M.S. Hapeez, N.R. Hamzah, H. Hashim, A.F. Abidin and M.K. Hamzah, "*An Algorithm for Identification of Different Types of Partial Discharge Using Harmonic Orders*", Przegląd Elektrotechniczny, R. 89 NR 5/2013, pp. 36-42. ISSN 0033-2097.

Mohammad Shukri Hapeez obtained his B. Sc. in Computer from the Uni-versity of Technology Malaysia in 2007 and his M.Sc. in Electrical Engineering from Universiti Teknologi MARA in 2011. Currently, completing his Ph.D in Electrical Engineering from Universiti Teknologi MARA, Malaysia. His research interests include computer, networking, interfacing, system identification, partial discharges and insulation materials.

Ngah Ramzi Hamzah obtained his Advanced Diploma in Electrical and Electronic Engineering from the Universiti Teknologi MARA in 1987 and his M. Sc. in Pulse Power Tech-nology from Strathclyde University, Glasgow, United Kingdom in 1992. In 2007, he received his PhD in Insulating Materials from University Malaya in Malaysia. His research interests include insulation, high voltage, partial discharges, insulation diagnostics and pulsed power. Currently, he is the Deputy Rector of Bertam Campus of Universiti Teknologi MARA, Pulau Pinang, Malaysia.

Habibah Hashim obtained her B. Sc. in Electrical and Electronic Engineering from the University of Nottingham in 1983 and her M. Sc. in Computer Aided Engineering from Teesside Polytechnic in 1986. In 2007, she received her PhD in Information and Communication Technology from Universiti Tenaga Nasional in Malaysia. Her research interests include computer and communication networks and data security and privacy. Currently she is the Deputy Dean of Research and Industrial Linkage in Faculty of Electrical Engineering, Universiti Teknologi MARA, Shah Alam, Malaysia.

Ahmad Farid Abidin received the B.E.E.S degree from University Kebangsaan Malaysia (UKM), Malaysia, in 2000, M.S.E.E. from Universiti Teknologi MARA (UiTM), Malaysia, in 2005 and PhD from Uni-versity Kebangsaan Malaysia (UKM), Malaysia, in 2011. He is currently a lecturer and Head of Power Department at the Faculty of Electrical Engineering, UiTM Shah Alam, Malaysia. His research interests are in application of signal processing in power system, power system protection and power quality.